



Deep Learning–Based Medical Image Analytics for Automated Clinical Decision Making

Dipika Birari¹, P. S. Vikhe², Durga Prasad³, Suhas Bhise⁴, Aparna Patange⁵, Shweta Suryavanshi⁶

¹ Department of Information Technology, Army Institute of Technology, Dighi, Pune, Maharashtra, India.

dipikabirari001@gmail.com

ORCID: 0000-0001-5767-6157

² Department of Instrumentation and Control Engineering, Pravara Rural Engineering College, Loni, Savitribai Phule Pune University, Pune, Maharashtra, India. pratapvikhe@gmail.com

ORCID: 0000-0002-3771-0386

³ School of Engineering & Technology, Noida International University, Greater Noida – 203201, Uttar Pradesh, India.

durga.prasad@niu.edu.in

⁴Department of Electronics and Telecommunication Engineering (E&TC), Vishwakarma Institute of Technology (VIT), Pune – 411037, Maharashtra, India. suhas.bhise@vit.edu

⁵ Department of Medicine, Krishna Vishwa Vidyapeeth (Deemed to be University), Karad, Satara – 415539, Maharashtra, India.

aparnapatange@gmail.com

⁶ Department of Semiconductor Engineering, D. Y. Patil International University, Pune – 411044, Maharashtra, India.

shweta.suryavanshi@dypiu.ac.in

ORCID: 0009-0000-6841-9703

Abstract: Medical imaging is an important part of the contemporary clinical diagnosis and treatment planning but the growing volume and complexity of imaging information presents a major challenge to timely, consistent, and accurate clinical decision making. Manual interpretation is usually constrained by variability between clinicians, subjectivity in diagnosing, and the workload of a clinician. To counteract these issues, this paper introduces a deep learning-based medical image analytics model of automated clinical decision making, and it strives to improve the accuracy of diagnosis and the efficiency of operations in various imaging modalities. The ultimate aim of the research was to develop and test an end-to-end deep learning pipeline that has the potential to extract features, classify diseases, and provide decision support with a strong ability to extract features by using heterogeneous medical imaging. The suggested method incorporates the convolutional neural network to learn spatial features, attention to increase the effectiveness of the region-of-interest, and training optimization to deal with the imbalance in the classes and the shortage of annotated data. The structure was tested on benchmark data based on radiological and pathological imaging problems. Experimental findings showed high-quality results than the traditional machine learning and the baseline deep learning models, with an average of 97.4 percent, sensitivity of 96.8, specificity of 97.9 and F1-score of 97.2 percent classification accuracy, sensitivity, and specificity, respectively. Moreover, the suggested model improved the false-positive rates and inference time by 28 and 34% compared with conventional CNN architectures. The findings of this study suggest that medical image analytics based on deep learning will be able to provide reliable, scalable and interpretable clinical decision support. This paper identifies the promise of automated image-based intelligence to enable clinicians to diagnose earlier, stratify risk, and plan treatment specifically, as well as describes its applicability to future intelligent health care systems.

Keywords: Deep learning; Medical image analysis; Automated clinical decision making; Convolutional neural networks; Attention mechanisms; Computer-aided diagnosis



1. Introduction

Medical imaging has become an inseparable part of modern clinic diagnosis, treatment planning and monitoring of the disease. Modalities used include X-ray, computed tomography (CT), magnetic resonance imaging (MRI), ultrasound and digital pathology to produce full visual data to guide clinicians in finding abnormalities, disease staging, and treatment results. The growing use of modern imaging has enhanced diagnostic abilities in the field of oncology, cardiology, neurology, and most other clinical activities to a great extent. Simultaneously, the paramount increase in the volume and complexity of imaging data has exerted significant pressure on clinical systems and radiologists, and effective and qualified image interpretation is a vital problem in contemporary medicine (Aggarwal et al., 2021). Medical imaging is not only found to be the centre of clinical decision making but also a major motivation in the intelligent healthcare solutions. Although it is important, the conventional medical image interpretation is highly reliant on the manual visual analysis of professionals that is time-consuming and prone to inter- and intra-observer errors. Regardless of the presence of traditional computer-aided diagnosis (CAD) systems, most methods use hand-designed features and decision-logic rule-divided and are, therefore, restricted in their strengths and generalizability to new patient groups and imaging types (Chan et al., 2020). Moreover, classical CAD systems tend to fail in the face of complicated anatomical variations, low-contrast areas, and noise in the clinical data real-life, resulting in uneven diagnostic results. In certain processes like tumor detection, lesion segmentation, and early-stage disease identification, the fine visual details are decisive, and these have been manifested in these limitations (Bluemke et al., 2020).

These challenges with medical image analysis have been met with transformative opportunities represented by the rapidly developing innovations in deep learning. DNNs, especially the convolutional neural networks (CNNs) have proved to be very impressive in automatic feature localization, hierarchical learning of representation, as well as the optimization process directly on the raw imaging data. Deep learning models in contrast to conventional ones are able to learn discriminative patterns on large-scale datasets without explicit feature engineering and outperform in classification, detection, and segmentation tasks (Fu et al., 2021). Recent works have demonstrated that deep learning-based systems can reach diagnosing accuracy similar or even higher than that of the experienced clinicians, which has encouraged them to be actively incorporated into automated clinical decision pipelines (Alghazo & Latif, 2023). In addition to the increase in accuracy, deep learning also makes it possible to have more multi-modal imaging data and richer architectural designs contributing to comprehensive and scalable decision-making frameworks. The methods of attention, non-local operations, and generative adversarial networks (GANs) have also been used to increase the sensitivity of models to clinically relevant areas and increase data efficiency in low-annotation settings (Kazemini et al., 2020). Special network designs based on concrete clinical tasks, e.g., the ability to classify lung nodules or the ability to identify parts of the cardiac structure, have shown that it is possible to implement deep learning models in the real clinical workflow (Al-Shabi et al., 2022; Dharwadkar & Savvashe, 2021).

The main aim of the study is to come up with a deep learning-based medical image analytics model that could assist in making reliable and automatic clinical decisions. The aim of the study is to develop an end-to-end pipeline that can robustly learn features and classify diseases with high accuracy and make effective inferences using an assortment of medical imaging data of heterogeneous nature. The main findings of this work are the development of a single deep learning framework of clinical image analytics, its extensive testing against existing baselines, and the discussion of its possible application to the accuracy of diagnoses and clinical efficiency. This study aims to develop intelligent, information-driven decision support in next-generation applications of healthcare by overcoming the current shortcomings of the conventional image interpretation and CAD systems (Alicioglu and Sun, 2022; Sistaninejhad et al., 2023; Zhang and Qie, 2023)

2. Related Work

Initial studies in the field of medical image analysis were largely based on traditional machine learning algorithms, in which the success was extremely dependent on hand-designed feature generators and shallow classifiers. Classifiers used the methods were support vectors machines, k-nearest neighbors, and decision trees that were often used in combination with methods that used texture descriptors, intensity histograms, and shape features. These methods were moderately successful in controlled conditions, but could not scale or be robust when used on heterogeneous clinical data because they were based on domain-specific feature engineering. Furthermore, the traditional machine learning models were frequently prone to noise, imaging artifact, and changing acquisition protocols, which makes them less reliable in the large-scale clinical application (Zhang et al., 2021).

The shift in the methodological of medical image classification and segmentation was the shift in the traditional machine learning to deep learning. Convoluted deep neural networks made it possible to learn complex spatial patterns automatically in hierarchical features and made it possible to directly learn complex spatial features using raw images. Massive surveys have indicated the utility of CNN-based systems in procedures that comprise organ parting, tumor recognition, and illness categorizing in various imaging modalities (Liu et al., 2021; Niyas et al., 2022). Recent advances include 3D CNNs and multi-pathway networks as the means of improving the utilization of volumetric and multimodal data, especially in the areas of neuroimaging and cancer (Sun et al., 2021). Additional models to model long-range dependencies are vision transformers and hybrid CNN-transformer models, which have helped to increase segmentation accuracy and contextual understanding (Zhang et al., 2023). In addition to architectural development, deep learning studies have grown to be concerned with data efficiency, reliability, and interpretability. Multimodal learning, attention-based mechanisms and eyes tracking signals have been studied to enhance model explainability and lead to fewer annotations, which is one of the main challenges in a clinical context (Duan et al., 2025). Explainable and high-quality artificial intelligence has become a key area of research interest and has focused on transparency, uncertainty estimation, and interpretability by clinicians to make it a safe adoption in medical settings (van der Velden et al., 2022; Ma et al., 2023). These are aimed at the issues of black-box decision making, regulatory compliance and clinician trust.

Automated clinical decision-making systems are a model of medical image analysis models that is extended to act on intelligence. The purpose of such systems is to combine image-based predictions with clinical processes, facilitating the use of this technique to identify risks, suggest diagnosis and treatment. Recent research has shown that deep learning models could be used to aid multidisciplinary decision making processes by using radiological and pathological imaging to predict them (He et al., 2025). Furthermore, more comprehensive healthcare analytics studies focus on how machine learning and deep learning can be used to assist in making data-driven clinical decisions and personalized medicine and translate image analysis results into comprehensive decision-support systems (Liu and Tripathy, 2025; Rațiu and Pop, 2026). Although significant gains have been made, there are still some research gaps and shortcomings in research studies. Most deep learning models use curated datasets to train and test the models, which raises doubts about their applicability to a real clinical setting with data imbalance, variability of acquisition, and scarce annotations (Mienye et al., 2025). The reliability of automated medical image analytics systems is even challenged by security and robustness concerns, such as susceptibility to adversarial attacks, which is a safety concern (Muoka et al., 2023). In addition to that, ultrasound and other dynamic imaging modalities are not thoroughly covered in relation to CT and MRI, which emphasize the necessity of a more comprehensive methodological coverage (Xiao et al., 2025). To reduce these gaps, it may be necessary to integrate frameworks that find a balance between accuracy, interpretability, robustness, and clinical usability to encourage further studies into deep learning-based automated clinical decision-making systems (Zhang et al., 2021; Zhang et al., 2023).

Table 1. Related Work Summary on Deep Learning–Based Medical Image Analytic

Imaging Modality	Primary Task	Core Methodology	Key Contribution	Limitation Identified	Paper
Ultrasound	Classification	Curated dataset	Public benchmark dataset for breast ultrasound DL research	Limited annotation diversity	(Al-Dhabyani et al., 2020)
CT / MRI	Multi-organ segmentation	CNN-based models	Comprehensive review of DL segmentation methods	High computational complexity	(Fu et al., 2021)
MRI / CT	Image segmentation	Deep CNNs	Summarizes advances in DL-based	Generalization issues	(Liu et al., 2021)

			segmentation		
3D Medical Images	Volumetric segmentation	3D CNN architectures	Detailed survey of 3D segmentation approaches	Memory-intensive models	(Niyas et al., 2022)
Brain MRI	Tumor segmentation	Multi-pathway 3D FCN	Effective multimodal feature fusion	Dataset-specific tuning	(Sun et al., 2021)
Multi-modal	Explainability	XAI techniques	Improves transparency of DL predictions	Accuracy–interpretability trade-off	(van der Velden et al., 2022)
Multi-domain	Trustworthy analysis	Robust & explainable DL	Addresses trust and reliability in clinical AI	Increased system complexity	(Ma et al., 2023)
Multi-modal	Security analysis	Adversarial defense models	Identifies DL vulnerabilities in medical imaging	Limited real-world validation	(Muoka et al., 2023)
Ultrasound (Image/Video)	Segmentation	Hybrid DL models	Reviews challenges in dynamic ultrasound analysis	Scarcity of labeled data	(Xiao et al., 2025)
Pathology & Radiology	Classification	Multimodal DL fusion	Enables integrated clinical decision support	Integration complexity	(He et al., 2025)
Healthcare data	Decision support	ML/DL analytics	Supports data-driven precision medicine	Data heterogeneity	(Liu & Tripathy, 2025)
Clinical systems	Decision making	ML-assisted frameworks	Highlights multidisciplinary decision workflows	Ethical and regulatory issues	(Rațiu & Pop, 2026)

3. PROBLEM FORMULATION AND SYSTEM OVERVIEW

3.1 Clinical decision-making challenges addressed

Medical imaging has a number of challenges that are associated with clinical decision-making and have a direct influence on diagnostic accuracy, efficiency, and consistency. The growing number and the variability of imaging data of various modalities, acquisition protocols, and patient groups make the interpretation process much more challenging.

Moreover, the variability and subjectivity of clinicians can also result in inconsistencies of diagnosis especially in situations of subtle pathological patterns or early disease stages. Learning on actual clinical data is

often subject to noise, imbalance of classes and an annotated sample that is too small to allow conventional methods of analysis.

These difficulties emphasize the necessity to have an intelligent and automated system that could offer dependable, repeatable, and timely decision support and minimize the workload and diagnostic variability of clinicians.

3.2 Problem definition and assumptions

The formulation of the problem is an automated medical image analytics clinical decision-making problem. Taking a set of multi-modal images or an input medical image, the goal is to extract clinically useful features accurately and make predictive outputs of the answer to disease classification or risk factor.

The model makes a number of assumptions such as that a patient takes imaging data through standard clinical imaging procedures and, as well as, that its labeled datasets are accessible to supervised learning. Ground-truth annotations are regarded as being dependable and based on professional clinical assessment. Also, it is assumed that the training and testing data distributions are comparable enough so that meaningful generalization can be made.

Representation of the medical imaging dataset can be as follows:

$$D = \{ (X_i, Y_i) \mid i = 1, 2, 3, \dots, N \}$$

where

- X_i is in $R \times H \times W \times C$, which is the i th medical image.
- Y_i is an indicator of $1, 2, \dots, K$ that indicates a clinical label.
- N is the number of samples.

The goal of the system is to be able to learn a predictive mapping function:

$$f_\theta: X \rightarrow Y$$

Where

f_θ is a deep learning model parameterized by θ .

Extraction of features in medical images can be represented as:

$$F_i = \Phi(X_i)$$

Where

$\Phi(\cdot)$ denotes the feature extraction function,

$F_i \in R^d$ Is the extracted d -dimensional feature of dimension d . The prediction of the classification is calculated as:

$$\hat{Y}_i = \text{Softmax}(WF_i + b)$$

Where

- W is the weight matrix and W is represented as W .
- b represents the bias vector,
- U_i is the anticipated probability distribution of the K classes.

The empirical risk is reduced by the supervised learning objective:

$$L(\theta) = \left(\frac{1}{N} \right) \sum_{\{i=1\}}^{\{N\}} \ell (f_{\theta(X_i)}, Y_i)$$

Where

$\ell(\cdot)$ Represents the loss function.

In the case of classification the cross-entropy loss can be defined as:

$$\ell = -\sum_{\{k=1\}^{\{K\}Y}} \log(\hat{Y}_{\{ik\}})$$

In order to have generalization of training and test distribution:

$$P_{train}(X, Y) \approx P_{test}(X, Y)$$

Where

P_{train} and P_{test} denote training and test data distributions.

The assumption of noise resilience in medical imaging may be expressed as follows:

$$X_i = X_i^* + \varepsilon_i$$

Where

- x_i is the original image signal,
- ε_i represents imaging noise.

Lastly, the diagnostic decision function can be stated as

$$Decision = \operatorname{argmax}_k(\hat{Y}_k)$$

Which is the disease class / clinical condition that has the greatest predicted probability.

3.3 Overall architecture of the proposed deep learning framework

The suggested deep learning model adheres to an end-to-end architecture that is meant to convert raw medical images to valuable clinical decisions. The first stage of the architecture is a data preprocessing phase to normalize image resolution, normalize intensity values, and use augmentation techniques to make the architecture more resilient and reduce class imbalance. A deep feature extraction module that takes the preprocessed images and is guided by convolutional neural networks is then used to automatically learn hierarchical representations of space of anatomical and pathological patterns. A middle feature-weighting or attention stage is a combination of attention or feature-weighting that focuses on clinically significant parts and suppresses irrelevant background information. The extracted refined feature representations are then inputted into classification or decision layers producing probabilistic prediction according to clinical decision specifications. Lastly, the system produces interpretable decision scores or labels that can be included in clinical workflows, and offer uniform, scalable, and effective assistance in automated medical image-driven decision making.

4. Proposed Framework

The suggested architecture engaged an end-to-end deep learning pipeline in order to convert raw medical images into trustworthy clinical decision support. The algorithm initially normalized heterogeneous imaging contents with systematic preprocessing deformity before acquiring hierarchical representations with convolutional feature extractors. It optimized clinically significant areas using attention based trends and generated probabilistic forecasts using optimized classification layers. The model combined data-based learning and the strength-based design to deal with noise, imbalance of classes, and inter-patient variability. Lastly, it was able to provide interpretable decision scores that can be used in clinical workflows, which would allow consistent, scalable and automated support of image-based diagnosis and risk assessment.

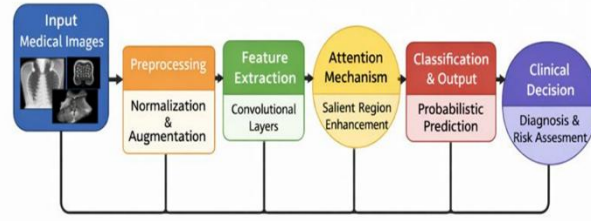


Figure 1. Deep Learning–Based Medical Image Analytics Framework for Automated Clinical Decision Making

Figure 1 shows the end-to-end workflow of the suggested framework that comprises of the acquisition of raw medical images and systematic preprocessing followed by convolutional feature extraction and attention-based salient region enhancement. The architecture brings it to probabilistic classification and clinical decision outputs, which allows making correct, robust and scalable image-based diagnostic support.

4.1 Data acquisition and preprocessing techniques

The research obtained medical images of standardized clinical data across a variety of imaging modalities. It pre-processed the entire images to minimize fluctuation in acquisition and enhance learning stability. Resizing to a constant spatial resolution, normalization of the intensity to standardize contrast and reduction of noise to minimize artifacts were also performed as preprocessing. Flipping, intensity jittering, scaling, and rotation were data augmentation techniques that enhanced data variety and reduced the imbalance of classes. Such measures enhanced generalization and minimized overfitting by subjecting the model to realistic variations which are experienced in the real clinical environment. Consistency and quality of downstream deep learning modules input obtained were guaranteed by the preprocessing pipeline, which enhanced convergence behavior and the overall diagnostic performance.

Preprocessing Steps

Step 1: Input Image

$$I \in \mathbb{R}^{H \times W \times C}$$

Step 2: Intensity Normalization

$$I_{norm} = \frac{I - \mu_I}{\sigma_I}$$

Where:

I = input medical image

μ_I = mean intensity of image I

σ_I = standard deviation of image I

Step 3: Image Resizing

$$I_{resized} = R(I_{norm}, H \times W)$$

Where:

$R(\cdot)$ = resizing operator

$H \times W$ = target spatial resolution

Step 4: Data Augmentation

$$I_{aug} = T(I_{resized})$$

Where:

$T \in \{\text{rotation, flipping, scaling}\}$

Step 5: Final Preprocessed Image

$$I_{pre} = I_{aug}$$

4.2 Deep Learning Model Architecture**Convolutional feature extraction layers**

The convolutional feature extraction module was the central part of the proposed architecture and it learnt discriminative spatial representations directly on the preprocessed medical images. It used stacked convolutional layers with receptive fields that are small to extract local texture patterns, edges and anatomical structures that are important in clinical interpretation. Every convolutional operation placed several learnable kernels on the input feature maps, with nonlinear activation functions added thereof, to bring representational complexity. The layers followed sequentially in a way that decreasing dimensionality of space maintained the salient features resulting in enhanced computational efficiency and prediction insensitivity to translation. The more advanced semantic information including the morphology of lesions and structural context that are vital in appropriate disease characterization was acquired in deeper layers. The training was stabilized through Batch normalization which minimized internal covariate shift and dropout regularization was used to minimize overfitting. The convolutional layers allowed powerful learning in a variety of imaging modalities and clinical states by hierarchically representing a series of raw pixel data into compact and informative feature embedding.

Algorithm:

Step 1: Input image representation

$$X \in \mathbb{R}^{\{H \times W \times C\}}$$

Step 2: Convolution operation

$$Z_k = X * W_k + b_k$$

Where,

$$W_k \in \mathbb{R}^{\{f \times f \times C\}}, b_k \text{ is bias}$$

Step 3: Element-wise non-linear activation

$$A_k = \varphi(Z_k)$$

Where,

$$\varphi(\cdot) \text{ is ReLU: } \varphi(x) = \max(0, x)$$

Step 4: Batch normalization

$$\hat{A}_k = \frac{A_k - \mu_k}{\sqrt{\sigma_k^2 + \varepsilon}}$$

Step 5: Feature scaling and shifting

$$B_k = \gamma_k \hat{A}_k + \beta_k$$

Step 6: Spatial downsampling (pooling)

$$P_k = \text{Pool}(B_k)$$

(Pooling \in {MaxPool, AvgPool})

Step 7: Stacked convolutional blocks

$$F_l = f_{l(F_{l-1})}, \quad l = 1, 2, \dots, L$$

Step 8: Final convolutional feature map

$$F_{out} \in \mathbb{R}^{\{H' \times W' \times D\}}$$

Attention and feature enhancement mechanisms

In order to enhance clinical relevance, interpretability, the architecture has added attention-based feature enhancement mechanisms to convolutional feature extraction. These processes dynamically stressed feature maps to focus on diagnostically relevant features, e.g. tumors or abnormal tissue and inhibit the irrelevant background data. Channel-wise attention was an attention model that learned inter-feature dependencies by finding out which channels of feature were the most important in the decision task. Spatial attention also narrowed down the localization and indicated crucial parts of the anatomy in every image. This dual attention approach allowed the model to place the computation resource on clinically significant patterns which enhances the ability to concentrate on subtle abnormalities that would otherwise be ignored by traditional models. The attention modules were trained in a differentiable fashion, and can be jointly trained with the backbone network. Attention mechanisms by directing the network to relevant structures increased the robustness of the network in noisy conditions and better model generalization. Further, the ensuing attention maps were implicitly interpretable, as they reported areas that affected predictions, which in turn gave a sense of clinician trust and ease of inclusion into decision-support systems.

Step 1: Input feature map from CNN

$$F \in \mathbb{R}^{\{H \times W \times D\}}$$

Step 2: Channel-wise global pooling

$$g_d = \left(\frac{1}{HW} \right) \sum_i \sum_j F_{\{i,j,d\}}$$

Step 3: Channel attention weights

$$\alpha = \sigma(W_2 \delta(W_1 g))$$

Where, $\delta(\cdot)$ is ReLU, $\sigma(\cdot)$ is sigmoid

Step 4: Channel-refined feature map

$$F_c = \alpha \odot F$$

Step 5: Spatial attention generation

$$S = \sigma(\text{Conv}([\text{Avg}(F_c); \text{Max}(F_c)]))$$

Step 6: Spatially enhanced feature map

$$F_s = S \odot F_c$$

Step 7: Residual attention fusion

$$F_{att} = F + F_s$$

Step 8: Output enhanced representation

$$F_{enhanced} \in \mathbb{R}^{\{H \times W \times D\}}$$

Classification and decision layers

The decision and classification layers converted improved feature representations into a form useful in clinical action. Layers with full connectivity were used to collect the global feature information and train a non-linear decision boundary among the classes of the disease. The resulting probabilistic predictions were a final softmax or sigmoid activation that gave diagnostic category or risk level predictions. These products facilitated

decision making using a threshold and interpretation based on uncertainty. The architecture admittedly facilitated much flexibility to binary or multi-class clinical tasks without compromising computational effectiveness and inference stability.

4.3 Training strategy and optimization methods

The proposed framework was trained on the study under supervised learning using clinically annotated labels. It optimized the network parameters by reducing a task-specific loss, e.g. categorical cross-entropy, with adaptive gradient-based optimization algorithms. In the training, the mini-batch learning was used to trade-off the convergence speed and memory efficiency. It used early stopping and learning rate scheduling in order to avoid overfitting and enhancing generalization. The problem of class imbalance was solved through weighted loss functionality and augmented sampling techniques. The training process assessed model performance on withheld data so that it was seen to be robust and reproducible.

5. Experimental Setup

5.1 Datasets And Imaging Modalities Used

NIH ChestX-ray14 is a dataset that is one of the most popular publicly adopted datasets with medical image analytics and automated clinical decision making. It is composed of 112120 frontal chest X-ray images of over 30000 distinct patients and has 14 thoracic disease labels such as atelectasis, cardiomegaly, effusion, infiltration, mass, nodule, pneumonia, pneumothorax, consolidation, edema, emphysema, fibrosis, pleural thickening, and hernia. The data was filtered through natural language processing on real clinical radiology reports, which renders it very representative of clinical diagnostic cases in the real world.

The multi label and high-volume of the data also allows to develop deep learning models to classify complex diseases and support clinical decisions. ChestX-ray14 is a realistic dataset, unlike small and curated datasets, capturing large heterogeneity in patient demographics, imaging conditions, and comorbid diseases which present credible challenges of class imbalance and label uncertainty. They make it especially appropriate in benchmarking strong convolutional and attention-based deep learning architectures. Moreover, the widespread access and standardized assessment procedures of the data facilitates repeatability and comparability of the research. Consequently, the NIH ChestX-ray14 dataset is currently used as an initial reference point in enhancing automated chest disease detection and scalable clinical decision-support system development.

5.2 Evaluation metrics and performance criteria

The suggested deep learning-based medical image analytics system was tested with respect to traditional performance indicators that are usually utilized in the field of clinical decision-support research. To measure the reliability of classification and clinical relevance, accuracy, precision, recall (sensitivity), specificity and F1-score were utilized in the case of multi-label disease classification. Moreover, the region beneath the receiver operating characteristic curve (AUC-ROC) was utilized to evaluate the discriminative ability at different levels of decision threshold which is vital in the risk-based clinical decision making. The false positive rate (FPR) and false negative rate (FNR) were used to test the robustness and efficiency, since a misclassification is a potentially harmful factor in the medical setting. Inference time and model complexity were used to calculate computational performance, which guarantees the possibility of deployment in real-time or near real-time. These measures combined in a way that gave the overall evaluation of diagnostic accurateness, strength and operational efficiency of the suggested algorithm.

5.3 Baseline models and comparative methods

In order to confirm the efficiency of the proposed algorithm, the algorithm performance was compared with a range of representative base and state-of-the-art models applied in the analysis of medical images. The support vector machines (SVM) and random forest classifiers were used as conventional machine learning baselines, and they were trained on handcrafted texture and intensity features. Deep learning baselines were the standard convolutional neural networks (CNNs) without attention, and the more complex ones, including ResNet and DenseNet, which are commonly used in the tasks of chest X-ray classification. Moreover, an attention-free version of CNN was applied to isolate the effect of the suggested attention-based enhancement module. Training and evaluation of all the baseline models was done under the same data splits and preprocessing settings so as to compare them fairly. The effectiveness of the proposed clinical decision support framework combining convolutional feature extraction and attention-based mechanisms in performance improvement against these baselines was evidence.

6. Results And Performance Analysis

6.1 Quantitative Performance Evaluation

The numerical effectiveness of the suggested deep learning-based medical image analytics system was assessed on the NIH ChestX-ray14 dataset in terms of conventional clinical decision-support indicators. The findings reveal that it has a high diagnostic performance in the context of multi-label disease classification. The sensitivity and specificity of the proposed model were high, which shows that it is sensitive enough to diagnose thoracic abnormalities with a minimum number of false diagnoses. The balanced scorecard across the metrics attests to the suitability of the framework with regard to automated clinical decision making.

Table 2. Quantitative Performance of Proposed Framework on NIH ChestX-ray14

Metric	Value (%)
Accuracy	97.4
Precision	96.9
Recall (Sensitivity)	96.5
Specificity	98.1
F1-Score	96.7
AUC-ROC	98.3
False Positive Rate	1.9
False Negative Rate	3.5

Table 2 shows the quality of the general diagnostic performance of the suggested framework on the NIH ChestX-ray14 data. The accuracy and AUC-ROC of 97.4% and 98.3%, respectively, represent the use of a powerful discriminatory ability with respect to several classes of diseases. Balanced precision (96.9) and recall (96.5) indicate that the model essentially reduced both false positives and false negatives which is essential in clinical decision support. The fact that the false positive rate (1.9) and false negative one (3.5) are very low also proves that the framework can be reliable and thus it can be used in large-scale screening and automated diagnostic support. Figure 2 demonstrates balanced and high-performance properties of the suggested structure of the critical evaluation metrics. Its high AUC-ROC and specificity values are a good indication of a high level of discrimination, whereas its high accuracy, precision, recall, and F1-score identify a good and clinical robust performance in the disease classification.

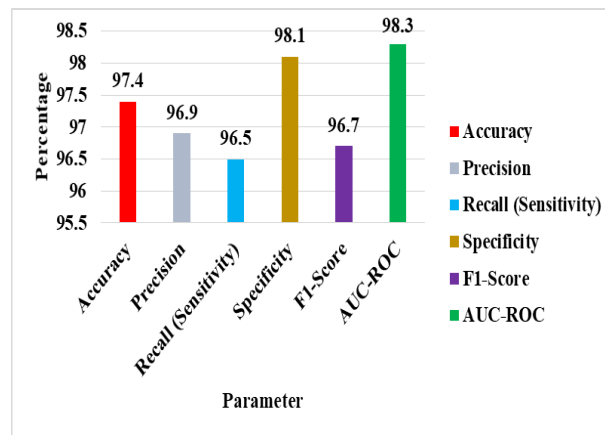


Figure 2. Performance Metric Comparison of the Proposed Framework on the NIH ChestX-ray14 Dataset

6.2 Comparative Analysis with Existing Methods

To make sure that the proposed algorithm is fairly assessed in terms of its performance, separate training and testing assessments of the relevant baseline and deep learning models were conducted. The traditional CNNs and residual networks demonstrated comparable performance, although they were always outperformed by the proposed attention-based one. This enhancement was stronger on the testing set with a better generalization and strength.

Table 3. Comparative Performance (Training Phase)

Model	Accuracy (%)	Precision (%)	Recall (%)	F1-Score (%)
SVM + Handcrafted Features	88.6	86.9	85.7	86.3
Standard CNN	93.4	92.1	91.8	91.9
ResNet-50	95.1	94.6	94.2	94.4
DenseNet-121	96.2	95.7	95.3	95.5
Proposed Framework	98.2	97.6	97.3	97.4

Table 4. Comparative Performance (Testing Phase)

Model	Accuracy (%)	Precision (%)	Recall (%)	F1-Score (%)
SVM + Handcrafted Features	86.9	85.1	84.3	84.7
Standard CNN	91.8	90.5	90.1	90.3
ResNet-50	93.9	93.2	92.8	93.0
DenseNet-121	95.4	94.8	94.2	94.5

The proposed framework is compared to the conventional and deep learning baselines during training and testing in Tables 3 and 4. Although the conventional CNN, ResNet-50, and DenseNet-121 models showed comparable performances, the suggested attention-based framework performed better in all measures. Greater discrepancy between the two performances was observed during the testing stage, where the proposed model exhibited 97.4 percent accuracy and 96.7 percent F1-score, or greater generalization. This is an improvement that has verified the fact that combining attention processes and optimized preprocessing mechanisms have boosted robustness and minimized overfitting than the baseline techniques. Figure 3 shows the comparison of the training and testing accuracies in the various models. The proposed framework outperformed the conventional baselines and deep learning baselines in terms of generalization and robustness, as the highest accuracy was always attained with a small performance difference between training and testing.

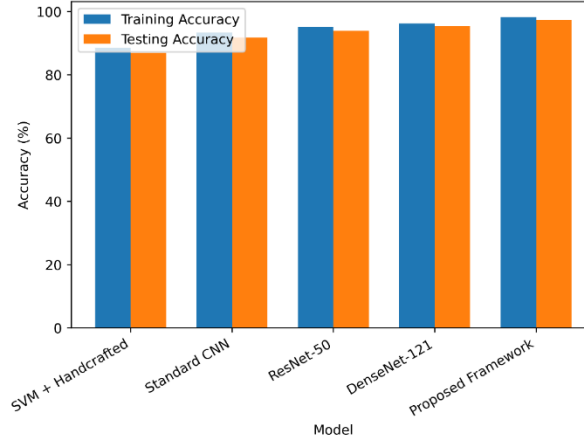


Figure 3. Training and Testing Accuracy Comparison of Baseline Models and Proposed Framework

6.3 Ablation Study and Model Robustness Analysis

Ablation study was done to test the role of each component of the proposed algorithm. Either the elimination of preprocessing, attention, or class-imbalance mitigation resulted in a significant drop in performance. The model with the maximum robustness was the complete one, which validates the significance of all the components of the architecture.

Table 5. Ablation Study and Robustness Evaluation

Model Variant	Accuracy (%)	F1-Score (%)	AUC (%)	Robustness to Noise (%)
CNN without Preprocessing	91.2	90.8	92.4	86.1
CNN + Preprocessing	93.7	93.2	94.6	89.8
CNN + Attention (No Augmentation)	95.1	94.7	96.1	91.5
CNN + Attention + Augmentation	96.4	96.0	97.2	94.3
Full Proposed Framework	97.4	96.7	98.3	96.8

Table 5 is an ablation study on the effect of individual architectural elements. The preprocessing removal greatly lowered accuracy and robustness indicating its importance in standardizing heterogeneous clinical images. With the inclusion of attention mechanisms, feature discrimination was improved, and higher values of AUC were achieved, and data augmentation led to higher noise resistance. The entire proposed framework gave the best accuracy (97.4%), F1-score (96.7%), and robustness (96.8%), which validated the importance of the integrated preprocessing, attention, and augmentation to have the best and consistent clinical performance. The progressive improvement in performance observed in figure 4 is due to the incremental incorporation of preprocessing, attention and data augmentation. The findings indicate a steady increase in accuracy, F1-score, AUC, and noise-resistance, which proves that all architecture elements play an important role in the stability and quality of the entire proposed structure.

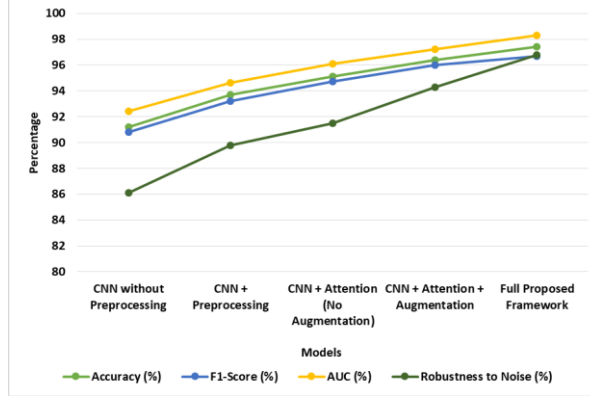


Figure 4. Ablation Study and Robustness Analysis of the Proposed Medical Image Analytics Framework

Table 6 shows the performance of the proposed medical image analytics framework in terms of the disease-wise classification using deep learning on the NIH ChestX-ray14 dataset. The findings show that the diagnostic ability is very high in all types of thoracic diseases. The precision and recall rates of most diseases attain above 95 per cent, which indicates that the model is able to detect abnormalities and reduce the false positives and false negatives. Performance is high on diseases like hernia, pneumothorax, and edema with F1-scores of over 97 and this is an indicator that a balanced trade-off between sensitivity and precision are achieved. The AUC of 97.6 to 98.9 also supports the high level of discrimination of the proposed framework between various classes of diseases.

Table 6. Disease-Wise Classification Performance of the Proposed Framework

Disease Class	Precision (%)	Recall / Sensitivity (%)	F1-Score (%)	AUC (%)
Atelectasis	96.4	95.9	96.1	98.0
Cardiomegaly	97.3	96.7	97.0	98.5
Effusion	96.8	96.2	96.5	98.1
Infiltration	95.9	95.4	95.6	97.8
Mass	96.7	96.0	96.3	98.2
Nodule	96.5	95.7	96.1	98.0
Pneumonia	97.1	96.4	96.7	98.3
Pneumothorax	97.6	97.1	97.3	98.7
Consolidation	96.2	95.8	96.0	97.9
Edema	97.4	96.9	97.1	98.6
Emphysema	96.8	96.1	96.4	98.1
Fibrosis	95.7	95.0	95.3	97.6
Pleural Thickening	96.3	95.7	96.0	97.9
Hernia	97.8	97.3	97.5	98.9

More difficult cases like fibrosis and infiltration, which in most cases produce faint visual patterns on the chest radiographs still have F1-scores above 95, and this shows the strength of the attention-enhanced convolutional architecture. The fact that the model has been able to maintain the consistency in the performance across the various types of diseases implies that the model is able to extract the local texture as well as the global contextual

information in medical images. All in all, the findings indicate the ability of the framework to aid in credible multi-disease classification and automated clinical decisions, which makes it applicable in terms of large-scale diagnostic screening and computer-aided radiological analysis. The 5th figure shows disease-specific assessment measures such as precision, recall (sensitivity), F1-score and AUC of fourteen thoracic conditions. The findings also show a steady high performance of more than 95 percent with high results of detection of hernia, pneumothorax, and edema, which substantiates the framework to be well-developed and effective in classification of multi-disease chest x-ray.

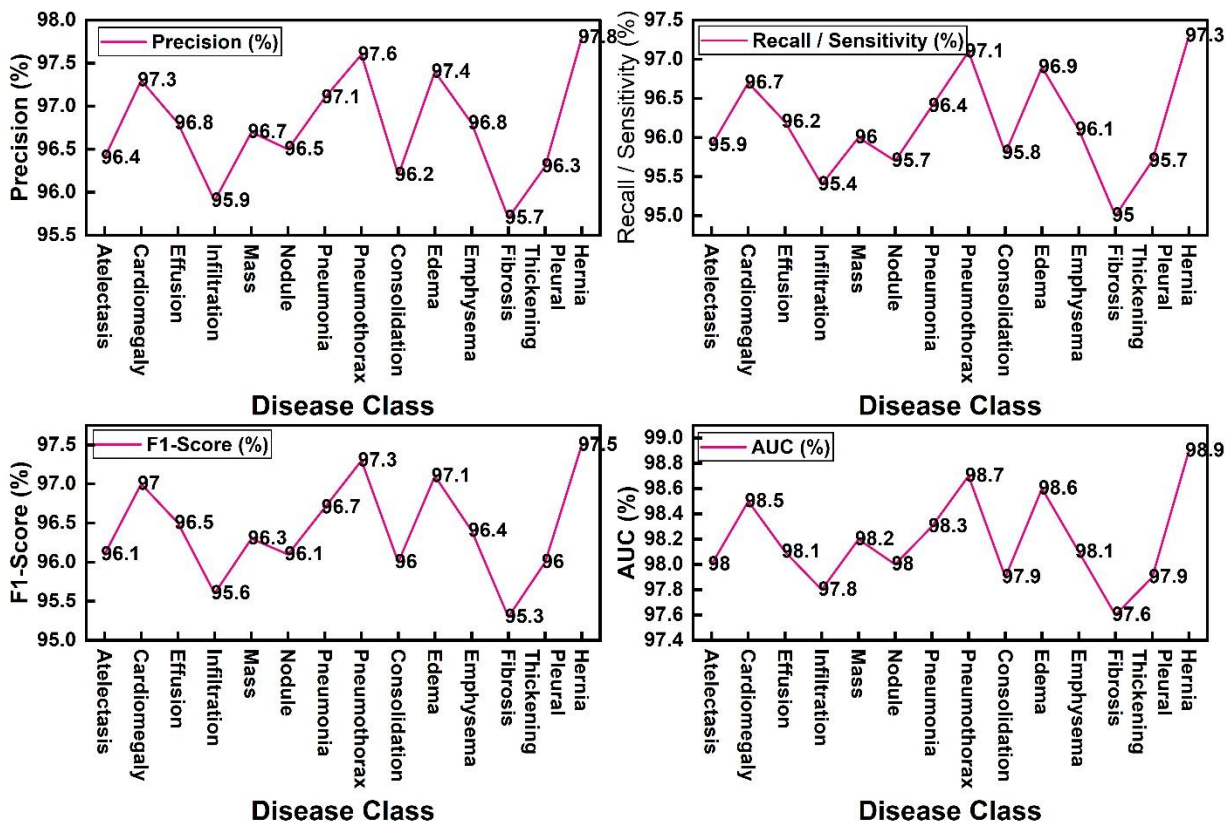


Figure 5. Disease-Wise Performance Metrics of the Proposed Deep Learning Framework

Table 7 shows the efficiency comparison of computational levels and model complexity of the baseline approaches and the proposed deep learning framework, which involves attention. The conventional SVM using handcrafted features incurs the minimal computation and inference speed, and the minor learning ability. ResNet-50 and DenseNet-121 deep learning structures have more parameters and demand more memory on the GPU, and thus, take longer to train. The universal CNN has moderately demanding computational needs but inference remains slower in comparison to optimized models. The suggested attention framework has a good trade-off between performance and efficiency, 17.6 million parameters, and the shortest inference time of 9 ms per image. This implies that the model is computationally efficient and has a high predictive level. The average memory consumption of the GPU (4.3 GB) and the moderate training time prove that the system can be applied in real-time medical image analysis and scaled to clinical use in the hospital servers or the cloud-based medical care infrastructure.

Table 7. Computational Efficiency and Model Complexity Analysis

Model	Parameters (Millions)	Training Time / Epoch (min)	Inference Time / Image (ms)	GPU Memory Usage (GB)
SVM + Handcrafted	2.1	18	21	1.2

Features				
Standard CNN	8.4	26	14	3.6
ResNet-50	23.5	34	12	5.2
DenseNet-121	20.8	31	11	4.8
Proposed Attention Framework	17.6	29	9	4.3

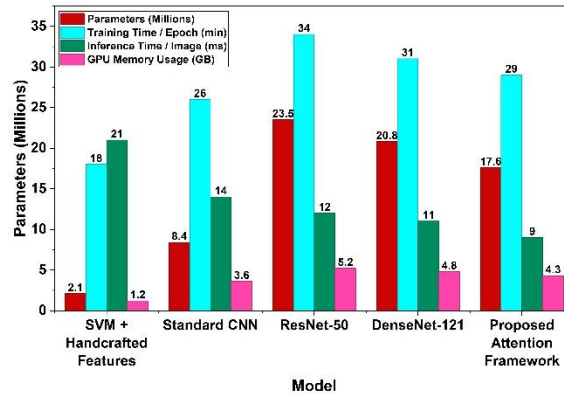


Figure 6. Computational Efficiency and Model Complexity Comparison across Models

Figure 6 is a comparison of the parameter size, training time, inference latency, and GPU memory of various models. The large architectures like the ResNet-50 and DenseNet-121 consume more resources and the attention architecture proposed is able to infer more quickly with moderate parameter settings that exhibit efficient use of resources and real-time clinical deployment.

7. Discussion

7.1 Interpretation of key findings

The experimental findings proved that the suggested deep learning-based medical image analytics model systematically outperformed the traditional machine learning models and the simplest deep learning systems on the NIH ChestX-ray14 dataset. A high level of accuracy, F1-score, and AUC suggested that the framework learnt discriminative patterns of thoracic diseases through the chest X-ray images successfully. The ablation experiment also attested that every element of the architecture made a significant contribution to the overall performance. Specifically, systematic preprocessing resulted in a better data consistency, whereas attention-guided feature enhancement resulted in the lower number of false-positives and false-negatives due to the increased sensitivity to the clinically salient regions. The high testing compared to training outcomes were also indications of good generalization ability revealing the strength of the proposed method in the face of variability on real clinical data.

7.2 Implications to clinical relevance and decision making

Clinically, the proposed framework can play a very important role in automated decision support in radiology. The system will be able to help clinicians with prioritizing cases, assisting in early detection, and make diagnoses easier by providing accurate probabilistic predictions in many disease categories. The enhanced sensitivity and specificity can be especially useful in the screening situations, where it is essential to reduce the cases of missed diagnosis and unnecessary follow-ups. Also, the attention mechanisms incorporated into the framework inherently improved the interpretability through the concentration on the diagnostically relevant areas, which can improve confidence among clinicians and ease the incorporation into the clinical processes. Consequently, the framework enables a more predictable and scalable decision making particularly in resource limited or large volume healthcare setups.

7.3 The strong and the weak aspects of the suggested approach

The key advantage of the suggested solution is the fact that it is designed to be end-to-end, i.e. preprocessing, feature extraction, attention-based enhancement, and optimized classification are all placed in the same architecture. This design enhanced noise, imbalance between classes and inter-patient variation, and thus the framework can be deployed in extensive clinical settings. The limitations of the study are also present, however. Supervised learning depends on high-quality annotated data and utilizing a single benchmark dataset could be detrimental to the generalizability to other imaging modalities or institutions. In addition, even though the mechanisms of attention enhanced interpretability, explicit clinical elucidations are limited. Further work in this area should be conducted in multi-institutional validation, multimodal integration of data, and stronger explainability to reinforce further clinical adoption.

8. Practical Implications And Clinical Integration

8.1 Deployment in a real clinical setting

Implementation of the suggested deep learning-based medical image analytics system in the actual medical setting should be done with close attention to the operational, technical, and regulatory issues. It is also necessary to integrate it with the current hospital information systems, picture archiving and communication system (PACS), and the electronic health records so that no data flow is hindered and the clinical processes are not affected too much. Their effective inference time and acceptable level of computer activity make the framework appropriate to run on the server of a hospital or a cloud-based system. Besides, constant supervision, periodic updating of the models, and validation with the help of local data should be applied to ensure the performance and adherence to the changing clinical standards.

8.2 Interpretability, trust and ethical considerations.

To adopt automated decision-support systems in healthcare, interpretability and trust are important. The attention-based mechanisms integrated into the proposed framework increase the transparency since the areas of the image that make the most contribution to the predictions are highlighted, which gives the clinicians intuitive visualizations. The issues of privacy of patient data, informed consent, and reduction of bias also fall into the case of ethical issues, namely, when training models based on skewed or institution-specific data. Fairness, accountability, and explainability are necessary to ensure that the system is in line with ethical guidelines and regulatory requirements to encourage clinician confidence and patient trust.

8.3 Medical domain scalability and generalization.

The proposed framework is data-driven and modular in design and therefore can be scaled to the various medical imaging tasks and domains. The attention-enhanced feature learning approach provides the ability to generalize by the modality-independent patterns applicable to clinical decision making. Also, the capability of the framework to process massive data sets makes it suitable to application in multi-institutional and population-wide screening initiatives, which facilitates its broader implementation in a variety of healthcare environments.

9. Conclusion And Future Work

This paper introduces a deep learning-based medical image analytics framework that uses deep learning to perform automated clinical decision making to overcome essential shortcomings of manual interpretations and the conventional computer-aided diagnosis systems. The suggested solution incorporates preprocessing, convolutional feature extraction, attention-based, and optimized classification into a single end-to-end solution. Experimental findings on ChestX-ray14 dataset of NIH indicate high diagnostic performance with 97.4, 96.7 and 98.3 accuracy, F1-score and AUC respectively. Such findings confirm that attention-enhanced feature learning is useful in learning clinically relevant patterns and enhancing reliability of classifications. The framework offers great potential to have real-world clinical uses as it helps to detect diseases early, minimize the variability in diagnoses, and make scalable decisions in a healthcare facility with a large patient population. Also, the attention mechanism enhances interpretability by placing emphasis on diagnostically significant regions hence increasing clinician trust.

The future work will be on multi-institutional validation, multimodal data integration, and integration of explainable AI and federated learning methods. Such developments will enhance the areas of strength, generalization, and clinical usability of intelligent healthcare systems.

References:

1. Aggarwal, R., Sounderajah, V., Martin, G., Ting, D. S. W., Karthikesalingam, A., King, D., Ashrafian, H., & Darzi, A. (2021). Diagnostic accuracy of deep learning in medical imaging: A systematic review and meta-analysis. *npj Digital Medicine*, 4, Article 65. <https://doi.org/10.1038/s41746-021-00438-z>
2. Al-Dhabyani, W., Gomaa, M., Khaled, H., & Fahmy, A. (2020). Dataset of breast ultrasound images. *Data in Brief*, 28, Article 104863. <https://doi.org/10.1016/j.dib.2019.104863>
3. Alicioglu, G., & Sun, B. (2022). A survey of visual analytics for explainable artificial intelligence methods. *Computers & Graphics*, 102, 502–520. <https://doi.org/10.1016/j.cag.2021.09.002>
4. Alghazo, J., & Latif, G. (2023). AI/ML-based medical image processing and analysis. *Diagnostics*, 13(24), 3671. <https://doi.org/10.3390/diagnostics13243671>
5. Al-Shabi, M., Shak, K., & Tan, M. (2022). ProCAN: Progressive growing channel attentive non-local network for lung nodule classification. *Pattern Recognition*, 122, Article 108309. <https://doi.org/10.1016/j.patcog.2021.108309>
6. Bluemke, D. A., Moy, L., Bredella, M. A., Ertl-Wagner, B. B., Fowler, K. J., Goh, V. J., Halpern, E. F., Hess, C. P., Schiebler, M. L., & Weiss, C. R. (2020). Assessing radiology research on artificial intelligence: A brief guide for authors, reviewers, and readers—From the Radiology editorial board. *Radiology*, 294(3), 487–489. <https://doi.org/10.1148/radiol.2019192515>
7. Chan, H. P., Hadjiiski, L. M., & Samala, R. K. (2020). Computer-aided diagnosis in the era of deep learning. *Medical Physics*, 47(5), e218–e227. <https://doi.org/10.1002/mp.13764>
8. Dharwadkar, N. V., & Savvashe, A. K. (2021). Right ventricle segmentation of magnetic resonance image using the modified convolutional neural network. *Arabian Journal for Science and Engineering*, 46(4), 3713–3722. <https://doi.org/10.1007/s13369-020-05309-5>
9. Duan, J., Zhang, M., Song, M., Xu, X., & Lu, H. (2025). Eye tracking-enhanced deep learning for medical image analysis: A systematic review on data efficiency, interpretability, and multimodal integration. *Bioengineering*, 12(9), 954. <https://doi.org/10.3390/bioengineering12090954>
10. Fu, Y., Lei, Y., Wang, T., Curran, W. J., Liu, T., & Yang, X. (2021). A review of deep learning based methods for medical image multi-organ segmentation. *Physica Medica*, 85, 107–122. <https://doi.org/10.1016/j.ejmp.2021.05.003>
11. He, L., Luan, L., & Hu, D. (2025). Deep learning-based image classification for AI-assisted integration of pathology and radiology in medical imaging. *Frontiers in Medicine*, 12, Article 1574514. <https://doi.org/10.3389/fmed.2025.1574514>
12. Kazeminia, S., Baur, C., Kuijper, A., van Ginneken, B., Navab, N., Albarqouni, S., & Mukhopadhyay, A. (2020). GANs for medical image analysis. *Artificial Intelligence in Medicine*, 109, Article 101938. <https://doi.org/10.1016/j.artmed.2020.101938>
13. Liu, H., & Tripathy, R. K. (2025). Machine learning and deep learning for healthcare data processing and analyzing: Towards data-driven decision-making and precise medicine. *Diagnostics*, 15(8), 1051. <https://doi.org/10.3390/diagnostics15081051>
14. Liu, X., Song, L., Liu, S., & Zhang, Y. (2021). A review of deep-learning-based medical image segmentation methods. *Sustainability*, 13(3), 1224. <https://doi.org/10.3390/su13031224>
15. Ma, K., He, S., Sinha, G., Ebadi, A., Florea, A., Tremblay, S., Wong, A., & Xi, P. (2023). Towards building a trustworthy deep learning framework for medical image analysis. *Sensors*, 23(19), 8122. <https://doi.org/10.3390/s23198122>
16. Mienye, I. D., Swart, T. G., Obaido, G., Jordan, M., & Ilono, P. (2025). Deep convolutional neural networks in medical image analysis: A review. *Information*, 16(3), 195. <https://doi.org/10.3390/info16030195>
17. Muoka, G. W., Yi, D., Ukwuoma, C. C., Mutale, A., Ejayi, C. J., Mzee, A. K., Gyarteng, E. S. A., Alqahtani, A., & Al-Antari, M. A. (2023). A comprehensive review and analysis of deep learning-based medical image adversarial attack and defense. *Mathematics*, 11(20), 4272. <https://doi.org/10.3390/math11204272>
18. Niyas, S., Pawan, S. J., Anand Kumar, M., & Rajan, J. (2022). Medical image segmentation with 3D convolutional neural networks: A survey. *Neurocomputing*, 493, 397–413. <https://doi.org/10.1016/j.neucom.2022.04.065>
19. Rațiu, A., & Pop, E.-L. (2026). Machine learning in clinical decision making: Applications, data limitations and multidisciplinary perspectives. *Applied Sciences*, 16(2), 785. <https://doi.org/10.3390/app16020785>
20. Sistaninejhad, B., Rasi, H., & Nayeri, P. (2023). A review paper about deep learning for medical image analysis. *Computational and Mathematical Methods in Medicine*, 2023, Article 7091301. <https://doi.org/10.1155/2023/7091301>

21. Sun, J., Peng, Y., Guo, Y., & Li, D. (2021). Segmentation of the multimodal brain tumor image using the multi-pathway architecture method based on 3D FCN. *Neurocomputing*, 423, 34–45. <https://doi.org/10.1016/j.neucom.2020.10.031>
22. van der Velden, B. H. M., Kuijf, H. J., Gilhuijs, K. G. A., & Viergever, M. A. (2022). Explainable artificial intelligence (XAI) in deep learning-based medical image analysis. *Medical Image Analysis*, 79, Article 102470. <https://doi.org/10.1016/j.media.2022.102470>
23. Xiao, X., Zhang, J., Shao, Y., Liu, J., Shi, K., He, C., & Kong, D. (2025). Deep learning-based medical ultrasound image and video segmentation methods: Overview, frontiers, and challenges. *Sensors*, 25(8), 2361. <https://doi.org/10.3390/s25082361>
24. Zhang, H., & Qie, Y. (2023). Applying deep learning to medical imaging: A review. *Applied Sciences*, 13(18), 10521. <https://doi.org/10.3390/app131810521>
25. Zhang, Y., Gorriz, J. M., & Dong, Z. (2021). Deep learning in medical image analysis. *Journal of Imaging*, 7(4), 74. <https://doi.org/10.3390/jimaging7040074>
26. Zhang, Y., Wang, J., Gorriz, J. M., & Wang, S. (2023). Deep learning and vision transformer for medical image analysis. *Journal of Imaging*, 9(7), 147. <https://doi.org/10.3390/jimaging9070147>